Welding of Cast Iron and Nodular Graphite Cast Steel. II : Arc-Welding of Nodular Graphite Cast Steel

著者	HOMMA Masao, WADA Tsuguyasu, YAMAYA Katsunobu
journal or publication title	Science reports of the Research Institutes, Tohoku University. Ser. A, Physics, chemistry and metallurgy
volume	12
page range	448-455
year	1960
URL	http://hdl.handle.net/10097/26999

Welding of Cast Iron and Nodular Graphite Cast Steel. II
Arc-Welding of Nodular Graphite Cast Steel*

Masao HOMMA, Tsuguyasu WADA and Katsunobu YAMAYA

The Research Institute for Iron, Steel and Other Metals

(Received Aug. 26, 1960)

Synopsis

The arc-welding of nodular graphite cast steel containing 1.2~1.5 per cent carbon and 1.8~2.8 per cent silicon was studied by the single-bead test and the tensile test with butt-welded specimens. The microstructures of weld metal and of heat-affected zone were examined by the single-bead tests by using cast iron and pure iron electrodes under the various preheats or post-weld annealings. The most remarkable difference of the microstructure from that of cast iron was the lack of ledeburitic layer in the heat-affected zone.

The tensile test with butt-welded specimens was carried out by using E7016, D4316(E6016), Ni-55 and cast iron electrodes. With post-weld annealing at 850°C, E7016 and D4316 could be applied with tolerable success. Ni-55 was also applicable even without annealing. The distribution of hardness and the microstructure were examined with the butt-welded specimens.

I. Introduction

Nodular graphite cast steel[1],[2] containing usually 1.2~1.7 per cent of carbon and 1~3 per cent of silicon has wide usability because of excellent mechanical properties and castability. The industrial utilities of this material and similar ones[3] are now in developing. This material contains spheroidal temper-carbon with the matrix of ferritic, pearlitic or bull's eye type, which can be controlled by the appropriate heat-treatments (Photo. 1). Though the structures and some

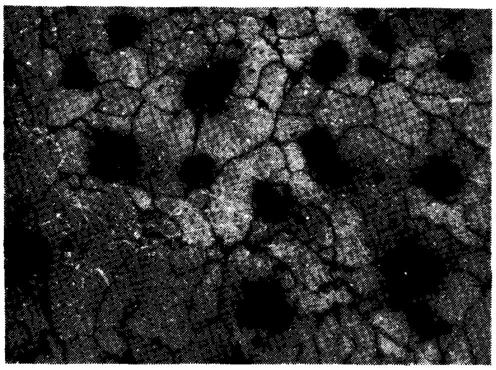
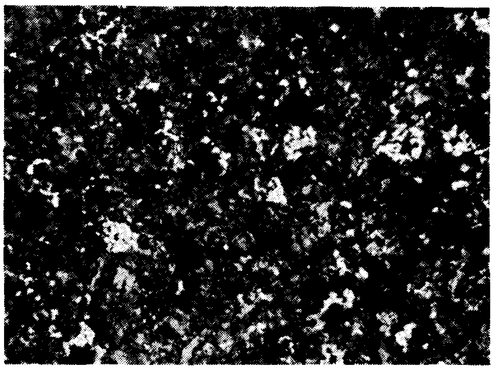

Photo. 1. Structure of base metal.
Left ; ferrite type. Right ; pearlite type. Nital etch ×120

* The 996th report of the Research Institute for Iron, Steel and Other Metals. Reported in Japanese in J. Welding Soc. Japan, (in press).

(1) M. Homma, Imono (Castings,) **31** (1959), No. 5, 1.
(2) M. Homma, H. Meguro, A. Minato and Y. Abe, Imono (Castings), **31** (1959), 9 ; Sci. Rep. RITU, **A12** (1960), 201.

properties are similar to those of nodular cast iron, this material may have somewhat improved weldability because of its relatively low carbon content. However, while the numerous studies[(4)~(9)] have been done on the welding of nodular cast iron, there is no report on the welding of this material.

Such being the case, the present study was carried out on microstructures and mechanical properties of arc-welded nodular graphite cast steel.

II. Materials

The chemical analyses and the mechanical properties of the nodular graphite cast steels are tabulated in Table 1. These materials were refined by Héroult furnace by using the reducing slag[(1)] and cast in the sand moulds. The dimensions of the moulds are shown in Fig. 1, in which 1-a and 1-b are those respectively for single-bead test and for butt welding. After the casting, the materials were heat-treated according to the standard procedure.[(2)] The specimens for the single-bead test were finished by grinding to remove the surface layer, and those for butt welding were mechanically shaped into the dimensions as will be stated below.

In Table 2 the properties of the commercial electrode used are tabulated.

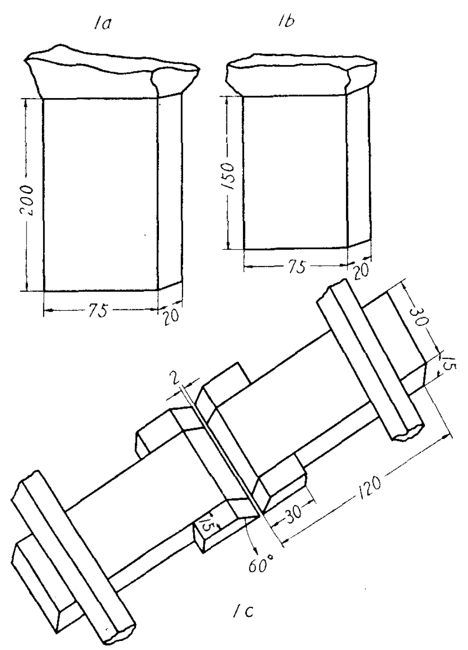

Fig. 1. Sand moulds and specimen for tensile test.

Table 1. Properties of base metals.

Charge No.	Chemical Analysis					Matrix	Mechanical Properties	
	C	Si	Mn	P	S		Tensile Strength	Elongation
1	1.25	2.28	0.25	0.11	0.013	Pearlitic	65.5 kg/mm²	—
2	〃	〃	〃	〃	〃	〃	75.0	—
3	1.45	1.86	0.51	0.036	0.049	〃	63.4	—
4	1.33	2.80	0.38	0.011	0.051	Ferritic	51.4	16%

(3) W. B. Larson, C. F. Joseph, F. J. Webbere and R. F. Thomson, Modern Castings, (1959), March, 47.
(4) E. E. Hucke and H. Udin, Weld. J., **32** (1953), 378-s.
(5) T. E. Kihlgren and H. C. Waugh, Weld. J., **32** (1953), 947.
(6) R. O. Day, J. S. Snyder and H. V. Inskeep, Weld. J., **36** (1957), 410-s.
(7) B. Townshend and E. O. Porter, Weld. J., **38** (1959), 329-s.
(8) R. C. Bates, Met. Prog., **76**(1959), 95.
(9) G. R. Pease, Weld. J., **39**(1960), 1-s.

Table 2. Electrodes used.

Name	Maker	JIS or AWS	Composition of Wire	dia (mm)	Coating
Pure Iron	T	—	Pure Iron	4	Carbon Type
Mild Steel	N	D4316	Mild Steel Class 1	4	Low Hydrogen
High Strength	K	E7016	C 0.06～0.11 Mn 1.00～1.30 Si 0.50～0.80	4	〃
Cast Iron	T	—	C 3.31 Si 3.70 Mn 0.49	4	Carbon Type
Ni55-Fe45	N	—	Ni 55～60 Fe 40～45	4	〃

III. Microstructure of single-bead tests

The microstructures of weld metal and heat-affected zone were observed by the single-bead test, which was the same as that mentioned in the preceding report. As the test plate, the ferritic one was used. The pure-iron and the cast-iron electrode were used to see the influence of the carbon content of electrode. The effects of the preheat and the post-weld annealing were also examined. The conditions of the tests and the results are summarized in Table 3.

Table 3. Conditions and results of experiments.

Current 135A

No.	Electrode	Preheat	Annealing (°C×hr)	Microstructure	
				D.M.	H.A.Z.
1	Pure Iron	—	—	Photo. 2	Photo. 3～5
2	〃	—	400×1hr	Sorbite	Photo. 6
3	〃	—	700×1hr	〃	Ferrite
4	〃	600°C	—	Sorbite	Sorbite
5	〃	〃	400×1hr	〃	〃
6	〃	〃	700×1hr	Ferrite	Ferrite
7	Cast Iron	—	—	Photo. 7	Similar to Photo. 4
8	〃	—	400×1hr	〃	Similar to Photo. 6
9	〃	—	700×1hr	Ferrite	Ferrite
10	〃	600°C	—	White Iron	Sorbite
11	〃	〃	400×1hr	〃	〃
12	〃	〃	700×1hr	Ferrite	Ferrite

Photos. 2 to 5 show the weld microstructures obtained by the use of pure-iron electrode without any preheat or annealing (Exp. No. 1 in Table 3). The deposited metal shows the acicular ferrite and troostite as shown in Photo. 2. The structure of the position very close to the fusion line in the heat-affected zone was martensite, (Photo. 3), whereas at the position somewhat apart from fusion line the boundary cementite accompanied by troostite was observed in the martensitic matrix (Photo. 4). In these zones, graphite nodules were almost dissolved in the matrix.

Photo. 6 shows the structure of the heat-affected zone annealed at 400°C, showing that the boundary cementite is not changed by annealing at such a temperature, while the martensite is converted into the tempered troostite. The decomposition of the boundary cementite was observed by the annealing at 700° (exp.

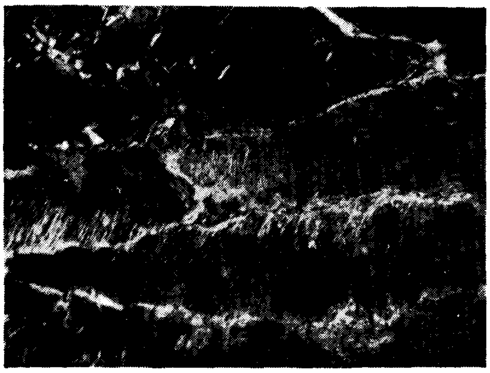

×120

Photo. 2. Deposited metal of sample No. 1.

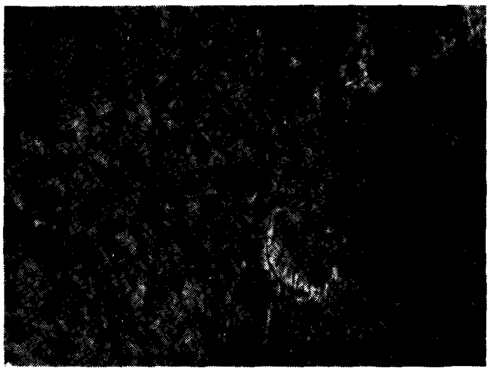

×120

Photo. 3. Fusion line of sample No. 1

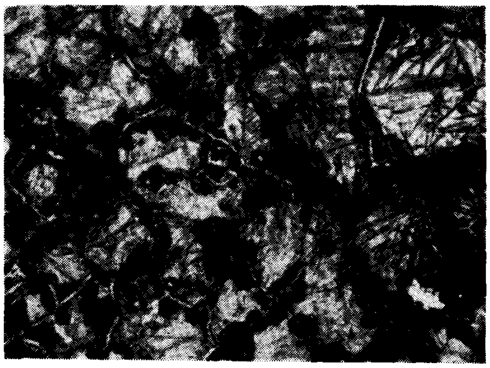

×120

Photo. 4. Heat-affected zone of sample No. 1.
Network cementite, troostite, and martensite.

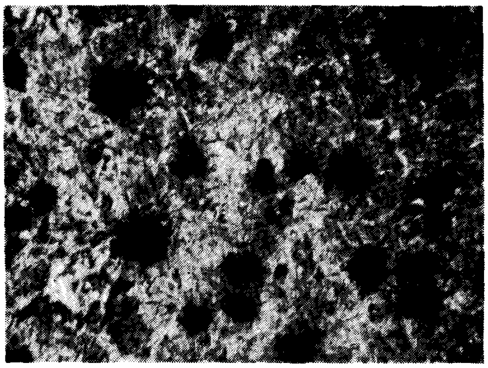

x×120

Photo. 5A. Heat-affected zone of sample No. 1.
Eutectoid matrix.

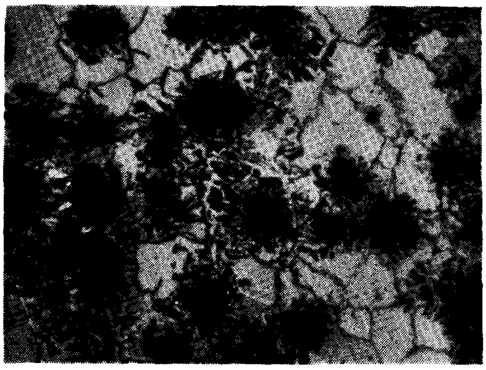

×120

Photo. 5B. Heat-affected zone of sample No. 2.
Hypo-eutectoid matrix.

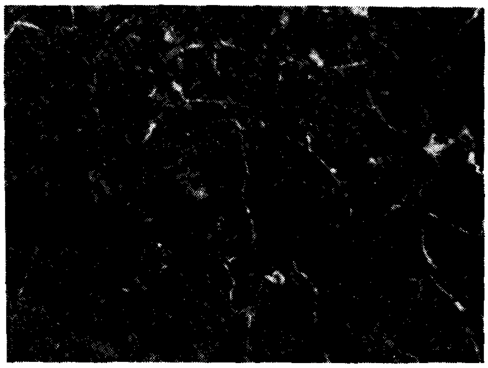

×120

Photo. 6. Heat-affected zone of sample No. 2. Network cementite and tempered troostite.

No. 3), in which the heat-affected zone became ferritic with the fine nodules of graphite. The deposited metal became sorbitic pearlite by these annealings.

In the case of the cast-iron electrode, on the other hand, some differences were observed in the boundary cementite of the heat-affected zone as well as the structure of the weld metals (Photo. 7), in comparison with those by the pure-

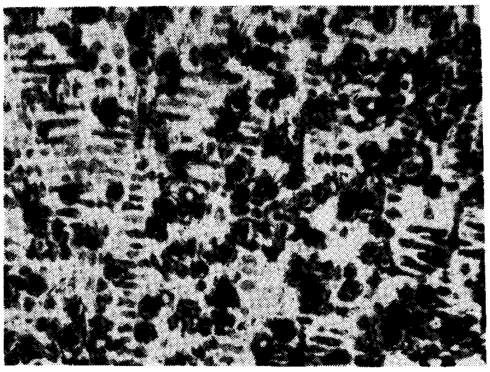

Photo. 7. Deposited metal of cast iron electrode.

iron electrode. Even in the position very close to the fusion line, an appreciable amount of boundary cementite appeared. The weld metal was of the structure of ledeburite.

In Exps. No. 4, 5, 6, and 10, 11, 12, the effects of preheats at 600°C were examined. When no post-weld annealing was applied, the weld metal and the heat-affected zone showed the sorbitic structure, except the weld metal by cast-iron electrode, where the ledeburitic structure was yet revealed. The annealing at 400°C showed practically no influence on the structures, and by the annealing at 700°C graphitization was completed even in the ledeburitic weld metal of cast-iron electrode, the matrix becoming ferritic in all cases. The fine nodules of graphite were also observed in the heat-affected zone of both electrodes, but its size was somewhat coarser than that in the case of no-preheat.

IV. Mechanical properties of butt welding

The tensile strength of butt-welded specimens was examined by using various electrodes and under different welding conditions. The specimens were fixed as shown in Fig. 1-c, and welded with seven-layers welding. The temperature of preheat was estimated by the thermopaints painted on the specimens. After the welding had been done, the side-plates were cut out, and without further shaping the tensile strength was measured.

The results are summarized in Table 4. In No. 7 in this table, the welded specimen was cooled in ash in order to reduce the cooling rate. The elongation was about 1 per cent for most specimens, though the values were not inserted in the table. One of the reasons for such a low elongation may be the condition of the post-weld annealing, which was not the ferritic annealing even for the ferritic specimens. Nos. 1～4 are the results in the case of high-strength steel electrode, E7016, showing practically no change in the strength with the temperature of preheats. When the mild-steel electrode was used, the strength was as

Table 4. Results of tensile tests.

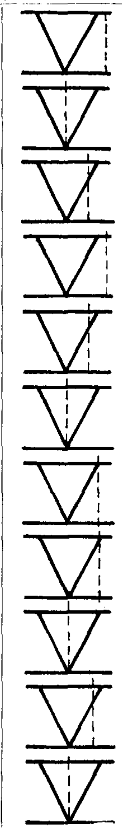

No.	Charge No.	Electrode	Welding Current	Preheat	Post-heat	Annealing	Tensile Strength	Fracture Location	Hardness Hv (500 g)		
									D.M.	Base	Max.
1	2	High Strength	150A	200°C	—	850°C × 2hr →A.C	40.3 kg/mm²	Base Metal	260	300	300
2	1	〃	〃	〃	—	〃	37.3	Weld	301	319	334
3	1	〃	177A	420	—	〃	38.9		212	287	285
4	1	〃	〃	〃	—	〃	38.9	Base Metal	248	316	300
5	3	Mild Steel	155A	200	—	〃	37.2		241	303	320
6	3	〃	〃	〃	—	〃	39.2	Weld	225	320	310
7	4	〃	120A	〃	Cool in Ash	—	34.9		236	228	360
8	4	〃	〃	—	—	850°C × 2hr →A.C	24.7		177	175	254
9	2	Ni55-Fe45	120A	—	—	—	35.0	Weld	202	293	405
10	2	〃	〃	—	—	—	28.0		200	333	416
11	1	Cast Iron	135A	200	—	850°C × 2hr →A.C	32.4	Weld	240	292	297

high as those of the high-strength steel electrodes.

In Fig. 2 the distributions of the hardness are shown for the butt-welding by using Ni–55 and high-strength steel electrodes. In the case of Ni 55, which was unannealed, it was microscopically observed that the high hardness of the heat-affected zone was due to the boundary cementite in the troostitic matrix. The next zone of this specimen, in which the hardness was about 400, was only of troostite.

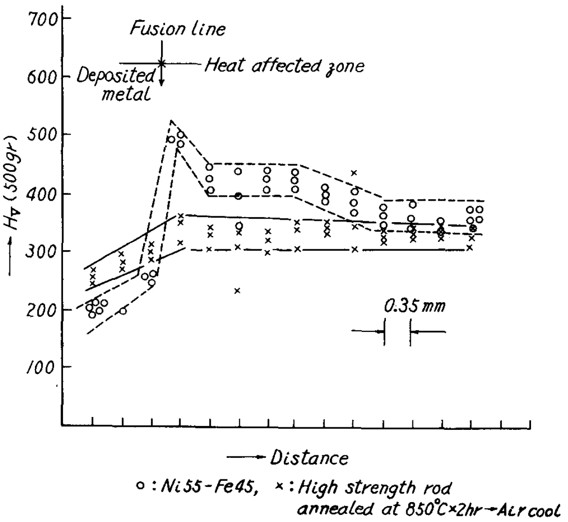

Fig. 2. Hardness distribution of heat-affected zone.

In the case of E7016, which was full-annealed at 850°C, there was no hard zone either in the heat-affected zone or the weld metal, the latter showing rather lower hardness than the parent metals.

The microstructure of the heat-affected zone in butt-welding was generally the sorbitic structure, as the full-annealing was applied in most cases. As the exceptions, however, in the case of Ni–55, which was unannealed, troostitic structure was shown accompanied by boundary cementite, and the case of ferritic parent metal ferritic structure was shown with the fine nodules of graphite (Photo. 8). Further, when the cast-iron electrode was used, the weld metal became the ferritic structure with eutectic graphite (Photo. 9).

×40

Photo. 8. Heat-affected zone of tensile test, sample No. 8.

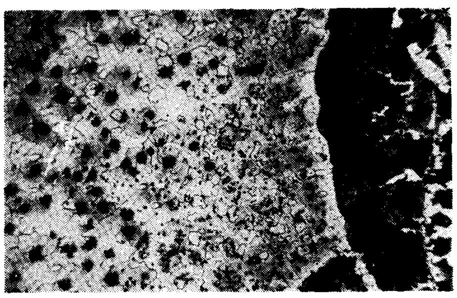

×120

Photo. 9. Deposited metal of tensile test, sample No. 11.

V. Conclusions

Most remarkable difference of the weld microstructure of nodular graphite cast steel from that of cast irons is the lack of ledebruitic layer. This may suggests more improved weldability of this material than that of the nodular iron or other cast irons. The boundary cementite, however, may somewhat easily be formed in the heat-affected zone, as the graphite in that zone is completely dissolved in the matrix. Thus, it is considered that the elimination of carbon from heat-affected zone occurs more effective than the cast irons. This is verified by the fact that the boundary cementite does not appear in the place very close to the fusion line, when the pure-iron electrode is used. This is considered as a result of decarburization.

By annealing at 850°C the boundary cementite is eliminated changing into fine nodules of graphite, but the shape is not completely spheroidal. Though the formation of the boundary cementite is undesirable, it is difficult to avoid it so far as the temperature of preheat is low.

The use of mild and high-strength steel electrode seemed to be of a tolerable success. This shows better weldability of this material than cast irons. Ni–55 electrode may also be applicable to this material as well as to the nodular iron or other cast irons. Other weldings especially the gas welding with similar-metal rods, which is often useful for cast irons, may be applicable. This will be investigated in the further works.

Summary

The arc-welding of nodular graphite cast steel containing $1.2\sim1.5$ per cent carbon and $1.8\sim2.8$ per cent silicon was studied by the single-bead test and by the tensile test with butt-welded specimens. The following results were obtained.

(1) No ledeburitic layer was observed in the heat-affected zone, which is the essential difference from that of the cast irons.

(2) The effects of preheats and post-weld annealings were studied. The boundary cementite in the heat-affected zone was completely eliminated by annealing at 850° or preheat at 600°. The fine nodules of graphite appeared in the heat-affected zone by these heat-treatments.

(3) The mild and the high-strength steel electrode, D4316 (E6016) and E7016, were applied with a tolerable success. Ni–55 electrode was also applicable without any post-weld annealing.